JOURNAL OF APPLIED POLYMER SCIENCE VOL. 17, PP. 1143–1164 (1973)

Thermosetting Reactions: Thermochemical Reactions of Triallyl Cyanurate and Triallyl Isocyanurate

J. K. GILLHAM and C. C. MENTZER,* *Polymer Materials Program, Department of Chemical Engineering, Princeton University, Princeton, New Jersey 08540*

Synopsis

Triallyl cyanurate (TAC) and triallyl isocyanurate (TAIC) are thermosetting monomers with interesting interrelations:

$$\text{TAIC} \xrightarrow{\text{R}\cdot} \text{poly(TAIC)} \xrightarrow{\Delta} \text{degradation}$$

$$\text{TAC} \xrightarrow{\sigma} \text{TAIC} \xrightarrow{\Delta} \text{poly(TAIC)} \xrightarrow{\Delta} \text{degradation}$$

$$\text{TAC} \xrightarrow{\text{R}\cdot} \text{poly(TAC)} \xrightarrow[\sigma]{\Delta} \text{poly(TAIC)} \xrightarrow{\Delta} \text{degradation.}$$

Calorimetry and infrared spectrophotometry were used to investigate the influence of atmosphere and initiator on the thermal events. The large extents of reaction observed during polymerization of TAC and TAIC are attributed to the formation of intramolecular rings. The higher conversions obtained with TAC are attributed to the extra length and flexibility of its allyl groups. Isomerization of poly(TAC) to poly(TAIC) is described as a three-step process: depolymerization of poly(TAC) to form monomeric TAC, isomerization of TAC to TAIC by a Claisen rearrangement, and repolymerization of the TAIC to poly(TAIC).

INTRODUCTION

Study of thermosetting processes and materials is neglected in polymer science and yet the problems posed are important and interesting. For example, even though the highly crosslinked polymers can be brittle and useless per se, fiber-reinforced composite materials which compete with steel for structural purposes involve these very polymers as matrices. In order to fabricate and understand the limits of thermal use of such systems, knowledge is needed of the thermal processes.

Triallyl cyanurate (TAC) and triallyl isocyanurate (TAIC) (Fig. 1) are liquid monomers which polymerize to form colorless, brittle, infusible, glass-like castings by thermosetting free-radical addition reactions. Poly(TAIC) is stable and mechanically rigid to above 400°C, whereas poly(TAC) undergoes exothermic reactions in the vicinity of 300°C which con-

* Present address: Polymers Department, General Motors Research, General Motors Technical Center, Warren, Michigan 48090.

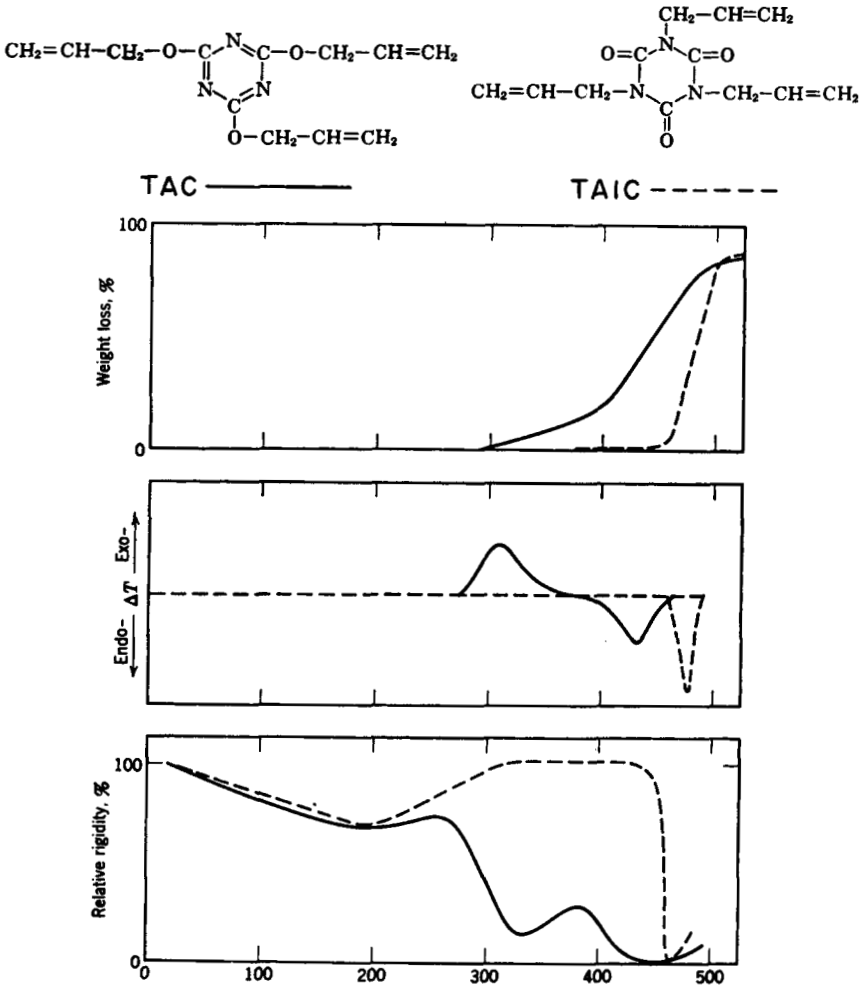

Fig. 1. Thermogravimetric, differential thermal, and thermomechanical analyses of poly(TAC) and poly(TAIC).[7] The polymers were made by heating monomer in nitrogen with 1.0% benzoyl peroxide at 95°C for 2 days. The thermomechanical behavior was obtained using torsional braid analysis.

vert poly(TAC) to poly(TAIC). The temperature-dependent behavior of crosslinked TAC and TAIC is shown in Figure 1 which includes the results of thermogravimetric (TGA), differential thermal (DTA), and thermomechanical analyses. The relationships may be summarized as follows:

The basis for the isomerization is the greater stability of the TAIC structure. The theoretical heat of combustion of a monomer is the sum of the contributions of individual bonds minus the resonance stabilization of the molecule. Since the products of combustion are the same for both molecules, the heat of isomerization is equal to the difference their heats of combustion. The resonance energy for the *s*-triazine ring is reported[1] to be 20 kcal/mole; that for the isocyanurate ring is not available but, assuming that the resonance arises from three amide groups,[2] the minimum resonance energy would be 51 kcal/mole. Neglecting resonance stabilization, the sum of the individual bond energies for TAC is 1656.1 kcal/mole and for TAIC is 1672.6 kcal/mole.[2] Therefore the calculated heat of combustion is 1636.1 kcal/mole for TAC and 1621.6 kcal/mole for TAIC. On this basis, TAIC is the more stable monomer by at least 14.5 kcal/mole.

This study, which provides the first detailed quantitative use in the field of polymerization reactions of du Pont's differential scanning calorimeter (DSC),[3] investigates further the solid state isomerization and investigates factors which affect the thermal events of allylic thermosetting polymerizations. The initial investigations of TAC, TAIC, and related materials are discussed by Clampitt et al.,[4–6] and a general review of allyl-*s*-triazine polymers is given by Gillham.[7]

EXPERIMENTAL

Theory and Procedure

The DSC cell was used to measure quantitatively the rate of heat generation resulting from the thermochemical reactions of TAC and TAIC. This calorimeter is simply a heated constantan disc incorporating two raised platforms upon which the sample and reference aluminum pans are placed. The disc acts as the primary means of heat transfer to the sample and reference pans. Embedded in the sample platform is a thermocouple. Connecting the two platforms is a differential thermocouple which measures their temperature difference (ΔT). The sample and reference platforms are calorimeters themselves which are programmed against each other in order to reduce or eliminate the heat loss factors which are inherent in all calorimeters. The recorded ΔT can be due to several factors. One is the heat capacity mismatch between the sample and reference. Another factor occurs when the sample is undergoing a thermal event. The equation for this instrument (see Appendix for development) is

$$\Delta T = (T_{RP} - T_{SP}) = R_C(C_S - C_R)\frac{dT_R}{dt} + R_C\frac{dh}{dt} - (R_C + R_S)C_S\frac{d(\Delta T)}{dt}$$

where T_{RP} and T_{SP} = reference and sample platform temperatures; C_S and C_R = sample and reference heat capacities; dT_R/dt = programmed heating rate; R_C = average thermal resistance of the constantan disc; R_S = thermal resistance between the sample pan and the sample platform;

dh/dt = rate of heat generation during a thermal event in the sample (− exothermic, + endothermic). The first term on the right-hand side of the equation is associated with the heat capacity mismatch, and the second term is associated with the thermal event occurring in the sample. The last term is due to the thermal lag which is inherent in all programmed calorimeters. This final term can be quite large during a rapid thermal event.

Measurement of the area under the ΔT-versus-T_{SP} curve for a thermal event is equivalent to integration of the above equation. The heat capacity term is either neglected or subtracted out.[8] The thermal lag term can be neglected since the response of the instrument (ΔT) before and after the thermal event is approximately the same (the limits of integration for the thermal lag term are the same). This means that the area under the curve ($\int \Delta T dt$) is directly proportional to the heat generated during the thermal event (ΔH), and the proportionality constant is R_C. R_C is the average thermal resistance of the constantan disc and varies with temperature; R_C was calibrated versus T_{SP} using the known heat capacity of Al_2O_3.[9] Sample size, programming rate, and shape of the pans also affect the calibration. Therefore, the calibration of R_C, and all experiments, were performed with a sample size of 4.0 to 8.0 mg, $\Delta T/\Delta t$ = 10°C/min, and (du Pont) hermetically sealed pans. Curves of ΔT versus T were changed to heat flux versus T by multiplying the ΔT by the calibration coefficient at the same temperature. Heat capacity effects of the sample and reference were removed[9]; therefore, only heat flux due to the reactions are shown. Each numerical result of Tables I and II is an average value obtained from at least four experiments.

Extents of reaction were determined calorimetrically by using −18.5 kcal as the heat of reaction of the polymerization of 1 mole of allyl groups. This is an average value for several different types of allyl reactions,[10] and it is a conclusion of the present report that this is indeed a good value. It yields a heat for complete polymerization for TAC and TAIC of −55.5 kcal/mole of monomer.

The calorimetric experiments were performed in nitrogen and in air. Air was present in only limited amounts since sealed pans were used.

Infrared analysis was used to monitor the thermochemical reactions by quenching from various temperatures ($\Delta T/\Delta t$ = 10°C/min) to room temperature. Each tabulated result represents the average of at least four experiments.

Materials

Since it is important that allyl monomers be pure for accurate investigation of reaction mechanisms, the analytically pure monomers were purified by passage through columns containing acidic and basic aluminum oxides. This was done in an attempt to ensure that there were no materials in the monomers which could initiate or inhibit the polymerization. Vapor-phase

TABLE I
Polymerization of TAIC-Calorimetric Results (Heats of Initiator Decomposition Removed)

Initiator level (atmosphere)	Heat of reaction, kcal/mole	Extent of reaction of allyl groups %
0.00% (N_2)	−26.6 ± 0.75	47.9
0.00 (air)	−27.0 ± 0.75	48.6
Lupersol 101		
0.25 (N_2)	−33.4 ± 0.85	60.2
0.25 (air)	−33.6 ± 0.85	60.5
0.50 (N_2)	−33.8 ± 0.85	60.9
0.50 (air)	−33.9 ± 0.85	61.1
0.75 (air)	−34.7 ± 0.85	62.5
1.00 (air)	−34.8 ± 0.85	62.7
3.00 (N_2)	−34.2 ± 0.7	61.6
3.00 (air)	−34.15 ± 0.7	61.5
5.00 (air)	−38.1 ± 1.0	68.6
10.0 (N_2)	−40.5 ± 0.85	73.0
10.0 (air)	−40.7 ± 0.85	73.3
BPO		
3.00 (N_2)	−30.8 ± 1.0	55.5
3.00 (air)	−30.2 ± 1.0	54.4
6.00 (air)	−33.3 ± 1.0	60.0
AIBN		
1.00 (air)	−28.8 ± 1.0	51.9
3.00 (N_2)	−31.9 ± 1.0	57.5
3.00 (air)	−32.1 ± 1.0	57.8

TABLE II
Polymerization of TAC—Calorimetric Results (Heats of Initiator Decomposition Removed)

Initiator level (atmosphere)	Heat of reaction (first peak), kcal/mole	Extent reaction of allyl group (first peak), %	Heat of isomerization (second peak), kcal/mole
0.00% (N_2)			−61.6 ± 2.3 (ΔH_{tot})
0.00 (air)			−60.6 ± 2.3 $(\Delta H)_{tot}$
Lupersol 101			
0.10 (N_2)			−63.0 ± 2.3 (ΔH_{tot})
0.25 (N_2)	−30.5 ± 0.9	55.0	−34.7 ± 1.05
0.25 (air)	−30.3 ± 1.1	54.6	−35.3 ± 1.2
0.50 (N_2)	−36.6 ± 0.9	65.9	−34.25 ± 1.05
0.75 (N_2)	−38.7 ± 0.9	69.7	−35.9 ± 1.05
1.00 (air)	−42.4 ± 0.9	76.4	−34.5 ± 1.05
3.00 (N_2)	−44.4 ± 0.8	80.0	−35.1 ± 0.95
3.00 (air)	−44.3 ± 0.9	79.8	−35.2 ± 1.05
5.00 (air)	−47.0 ± 1.1	84.7	−35.1 ± 1.2
10.00 (N_2)	−47.3 ± 1.1	85.2	−35.8 ± 1.2
10.00 (air)	−47.9 ± 1.1	86.3	−35.4 ± 1.2
BPO			
3.00 (air)	−32.8 ± 0.9	59.1	−35.7 ± 1.05
3.00 (N_2)	−32.9 ± 1.3	59.3	−35.4 ± 1.5
6.00 (air)	−40.4 ± 1.1	72.8	−34.1 ± 1.2

chromatography and infrared and nuclear magnetic resonance spectra were used for analysis, and in no case were any impurities detected in the monomers. The infrared and nuclear magnetic resonance spectra (Figs. 2 and 3) showed that the samples of TAC and TAIC were not mixtures of

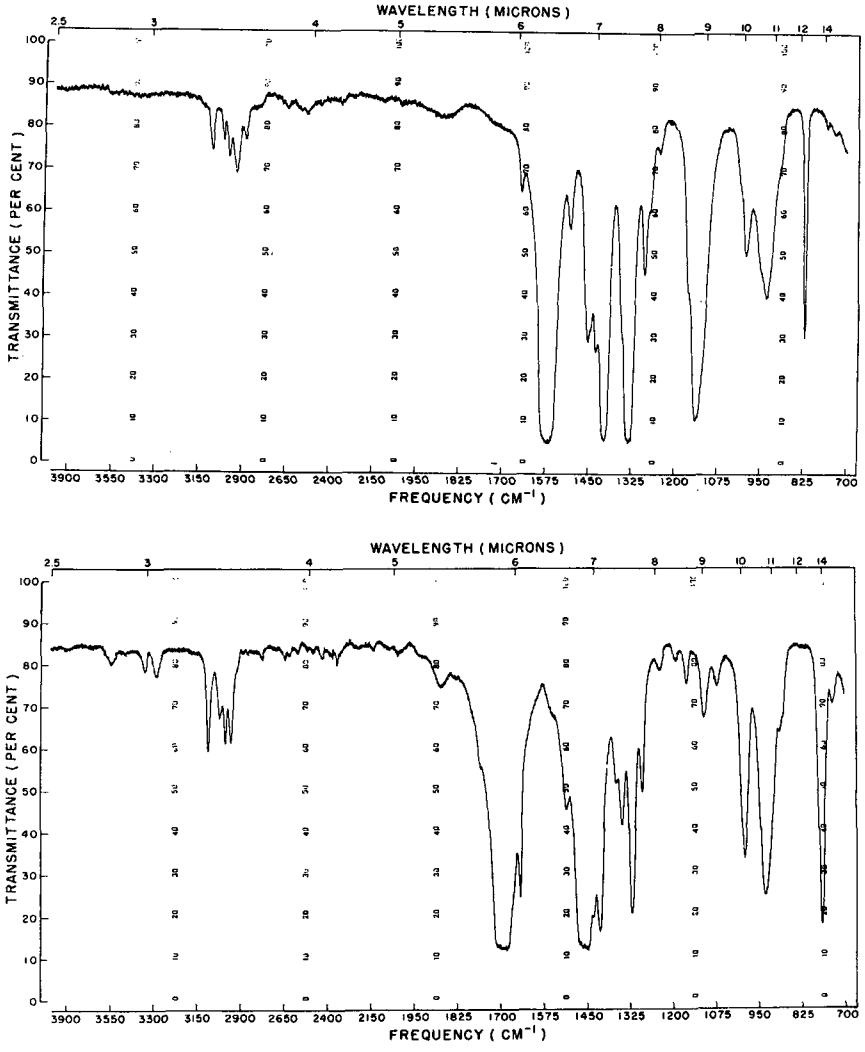

Fig. 2. Infrared spectra of pure triallyl cyanurate (top) and triallyl isocyanurate (bottom).

isomers. Experiments in nitrogen involved further purification by degassing to remove air. The initiators used were 2,5-dimethyl-2,5-bis(*tert*-butylperoxy)-*n*-hexane (Lupersol 101), 2,2-azobis-2-methylpropionitrile (AIBN), and benzoyl peroxide (BPO).

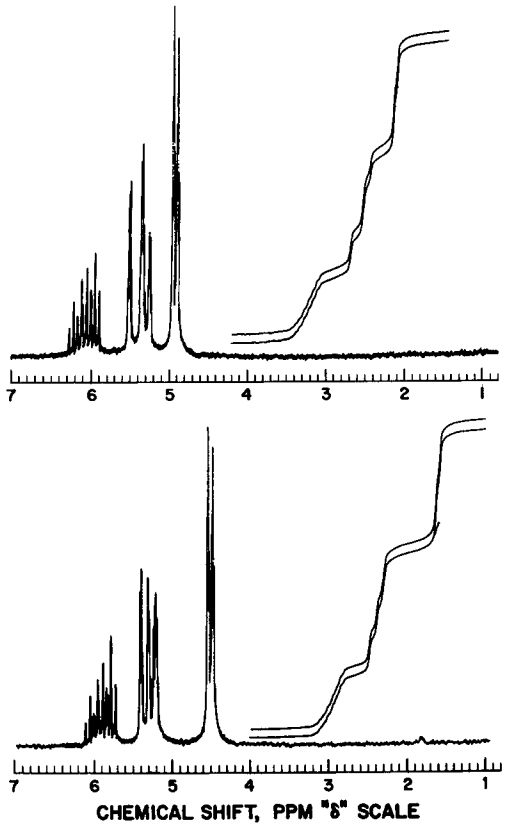

Fig. 3. 100 mHz NMR spectra of pure triallyl cyanurate (top) and triallyl isocyanurate (bottom).

RESULTS AND DISCUSSION

Polymerization in the Absence of Initiators

TAIC reacts in the absence of air in two steps (Fig. 4) which together involve −26.6 kcal/mole of heat and correspond to 47.9% reaction of the TAIC allyl groups. The heat generated during the first step accounts for 9% reaction of the allyl groups. The product of this first reaction step is a clear rubbery material (at 25°C) which contains 20% of material which is insoluble in benzene and chloroform. Assuming that only monomer is soluble, the amount of insolubles indicates that branching has occurred (no branches would result in 27% insolubles for 9% reaction). Gel formation in addition polymerization can occur at much lower conversions than in step-growth polymerization. This is a consequence of the addition-type mechanism which yields high molecular weight material at the beginning of reaction. This high molecular weight material has a high functionality of unreacted allyl groups, and therefore the probability of early branch formation is high.

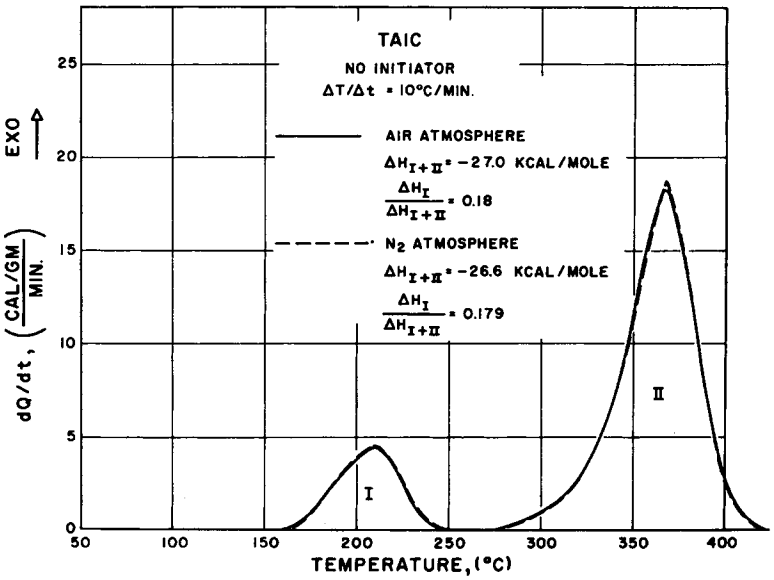

Fig. 4. Thermocalorimetry: polymerization of triallyl isocyanurate in the absence of initiator.

Addition of a limited amount of air to the TAIC does not affect the results. Both the shape of the curve and the overall extent of reaction remain the same. Addition of radical inhibitors (Ionol) eliminates polymerization of the allyl groups below 200°C.

The two step reaction of TAIC is interpreted by considering the mechanism of thermal formation of radicals. Radicals are formed by bimolecular collisions; the probability of radical formation is dependent on the number of collisions and the energy of those collisions. Formation of radicals results in polymerization. The overall degree of polymerization for allyl reactions is low due to termination of kinetic chains by reaction of radicals with allylic hydrogen to form terminated chains and stable allyl radicals. This means that reactive radicals must be continually generated in order to reach high conversions. As the gel point is reached, there is a sudden change in the rheological properties of the reacting system which causes a decrease in the number of bimolecular collisions which form radicals. This results in the observed slowing down of the polymerization, and higher temperatures are needed before radical formation again proceeds to an appreciable extent.

TAC (Fig. 5) reacts in the absence of air in two steps, but the first peak is small (and almost nonexistent in some runs). Both thermal events start and peak at lower temperatures than for TAIC. The total heat, −61.6 kcal/mole, includes both the heat of isomerization of the TAC structure to the TAIC structure and the heat of polymerization. Since the heat of isomerization is about −35 kcal/mole (see below), the total heat of polymerization for TAC (no air, no initiator) is approximately −27 kcal/mole,

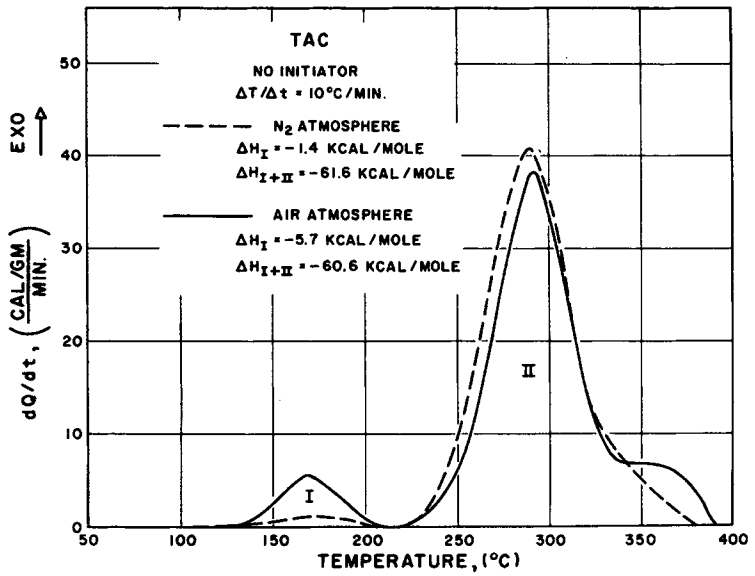

Fig. 5. Thermocalorimetry: polymerization and isomerization of triallyl cyanurate in the absence of initiator.

which corresponds to 48% reaction. This is the value obtained for the thermal polymerization of TAIC. Parallel studies in nitrogen with TAC using infrared spectra (Fig. 6) showed that, whereas no polymerization (reduction of the allyl 925 and 990 cm^{-1} bands) and no isomerization (disappearance of the C—O—C 1130 cm^{-1} and the *s*-triazine 815 cm^{-1} bands of the TAC, and appearance of the C=O 1700 cm^{-1} and the isocyanurate 750 cm^{-1} bands of the TAIC) occur on heating of the monomer to 210°C, heating to 390°C results in complete isomerization and appreciable disappearance of unsaturation.

The presence of a limited amount of air with TAC causes considerable change in the shape of the reaction curve (Fig. 5). The total heat remains the same, but there are two distinct reaction steps. Since infrared analysis shows that no isomerization occurs below 210°C, and since the first step could be eliminated by an inhibitor (Ionol), the heat generated in the first step is attributed solely to polymerization of TAC. The extent of reaction during this step is again 9%, indicating that the air- or oxygen-induced polymerization of TAC stops as the gel is formed. Oxygen-induced polymerization depends on the formation of hydroperoxides which readily decompose to form radicals. The hydroperoxides were not present in the TAC initially since degassing and performing the run in nitrogen removed this first reaction peak. The hydroperoxides are therefore formed during heating of the TAC in air. Oxygen is present dissolved in the TAC and also is present in the cavity above the monomer. Formation of a gel would severely restrict the diffusion of oxygen into the reacting system and thereby cause a reduction in the formation of the hydroperoxide. The pre-

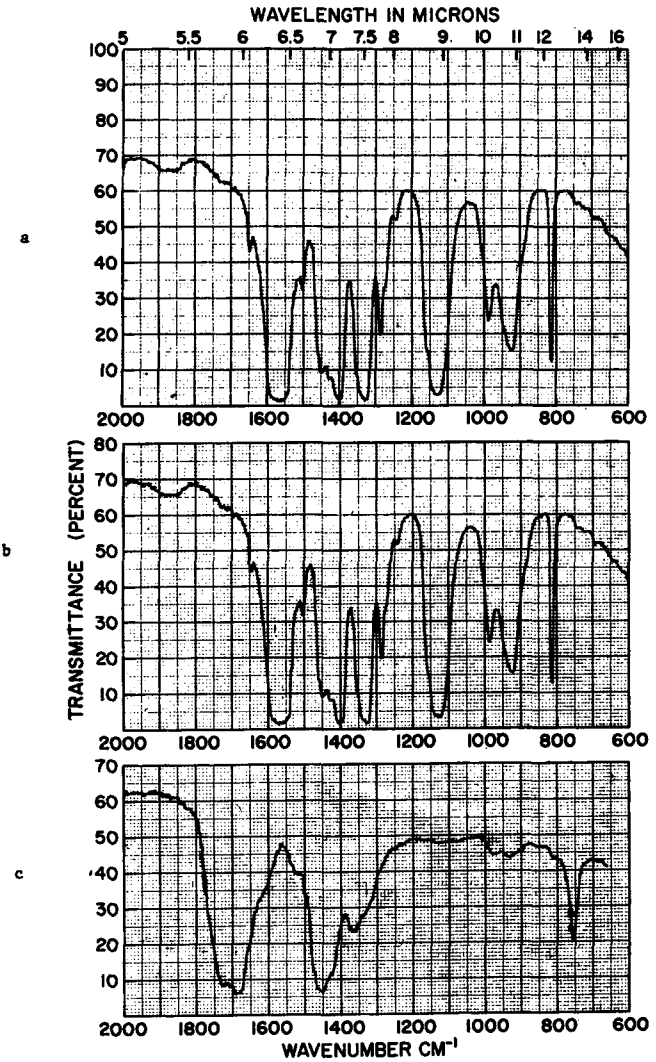

Fig. 6. Infrared spectra of TAC with no initiator (nitrogen atmosphere): (a) room temperature; (b) quenched from 210°C (note: no isomerization and very little polymerization); (c) quenched from 390°C (note: complete isomerization of TAC to TAIC with additional polymerization).

polymerization of TAC causes an upward shift in the second reaction step. A shoulder forms at 360°C which corresponds to the peak temperature of the second reaction step in TAIC. The polymerization of the TAIC (formed by isomerization of TAC) has been shifted to a higher temperature by the presence of a gel structure. It appears that in the absence of air, TAC isomerizes and the TAIC polymerizes in one thermal event. In the presence of air, some of the TAC prepolymerizes to poly(TAC) in a first step, which is followed by a second step which includes the isomerization

of TAC to TAIC and poly(TAC) to poly(TAIC), and the polymerization of TAIC.

The total extent of thermal polymerization for both TAC and TAIC is the same (−27 kcal/mole), and the net result in both cases is the polymerization of TAIC.

Radical-Induced Polymerization of TAIC

Table I summarizes calorimetric experiments made with TAIC. The heat of initiator decompositions were determined[9] and have been removed, and so the tabulated values are the heats of polymerization. Reactions using various concentrations of Lupersol 101, without and with air, are shown in Figures 7 and 8, where it is apparent that most of the reaction occurs in the vicinity of 175°C. The results are the same without and with the presence of air. At low (0.25% and 0.5%) initiator concentrations, some thermal polymerization continues until elevated temperatures, whereas with higher concentrations, reactions cease at lower temperatures. In the range 0.75% to 3.0% Lupersol 101, the total heat generated remains constant. Increasing the initiator concentration lowers the peak temperature. Further increases of the initiator concentration (5.0% and 10.0%) result in more heat being generated, and the shape of the reaction curve changes in that a shoulder forms after the main peak has been reached.

The type of initiator can have a considerable effect on the shape of the reaction curves and some effect on the heats generated (Fig. 9). Results in nitrogen and in air (not shown) are the same for initiators present at the

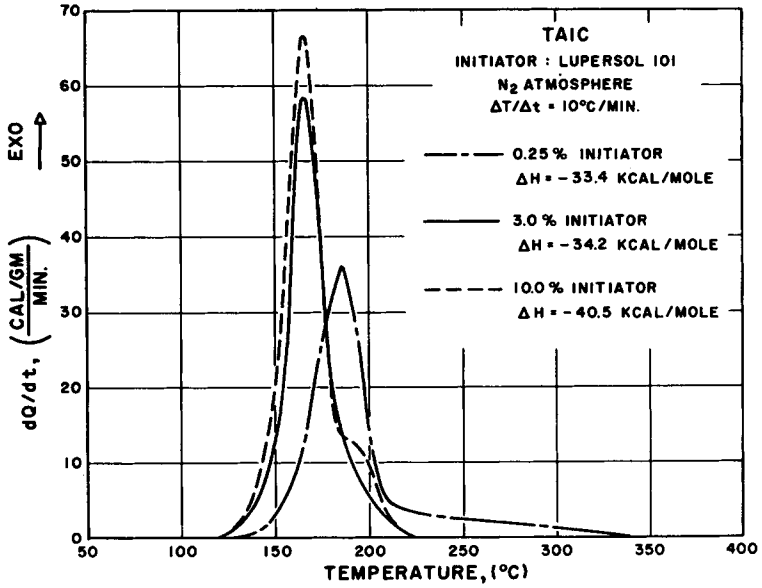

Fig. 7. Thermocalorimetry: polymerization of TAIC in nitrogen. Effect of initiator concentration.

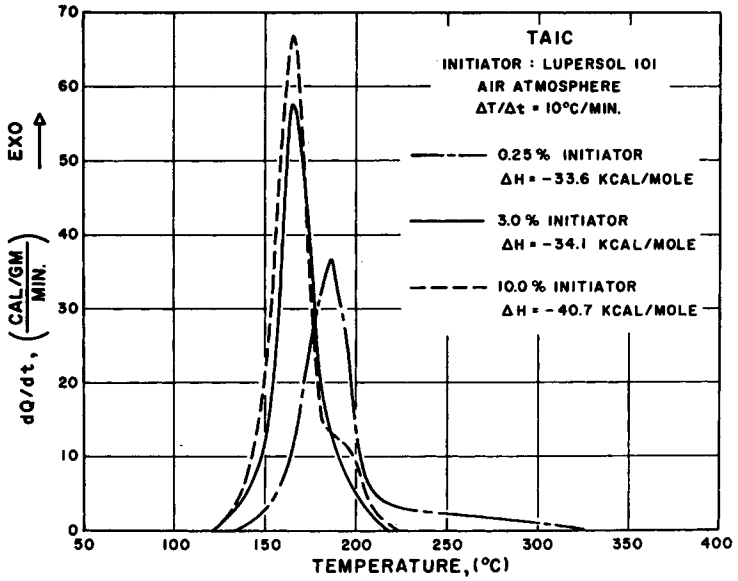

Fig. 8. Thermocalorimetry: polymerization of TAIC in air. Effect of initiator concentration.

3% level. Since AIBN and BPO start to decompose at a lower temperature than does Lupersol 101, the polymerization starts at a lower temperature. BPO seems to generate a more efficient radical for polymerization of TAIC than does AIBN in that more polymerization occurs while the initiator is present using BPO than when AIBN is used. These experiments were performed on a weight basis. Using a molar basis, AIBN was present in greater concentration than was BPO (AIBN, MW 164.2; BPO, MW 242.2). Initiation of polymerization occurs in two steps; the first is the formation of the radical, and the second is the reaction of the radical with a monomer to form an active site for polymerization. Both AIBN and BPO readily form radicals at the same temperatures, but the reactivity of the radicals must be different. Reaction of a radical with an allyl group leads to either an active site or an inactive allyl radical (extraction of a hydrogen atom by "allylic degradation"). A possible explanation for the low efficiency of the AIBN radical is that it more readily extracts hydrogen atoms than does the BPO radical.

It is difficult to compare the efficiency of Lupersol 101 with AIBN and BPO since it decomposes at a higher temperature where the kinetics of polymerization are more favorable. The first peak of the AIBN-initiated and the only peak of the BPO-initiated polymerizations are due to radical-initiated polymerization of the TAIC. Above 150°C, very little of the initiator is left; therefore, the additional polymerization which is observed for AIBN (second peak) is probably due to radicals that have been trapped in the polymer matrix. The continued reaction at higher temperatures for both AIBN and BPO is due to thermal induced polymerization of

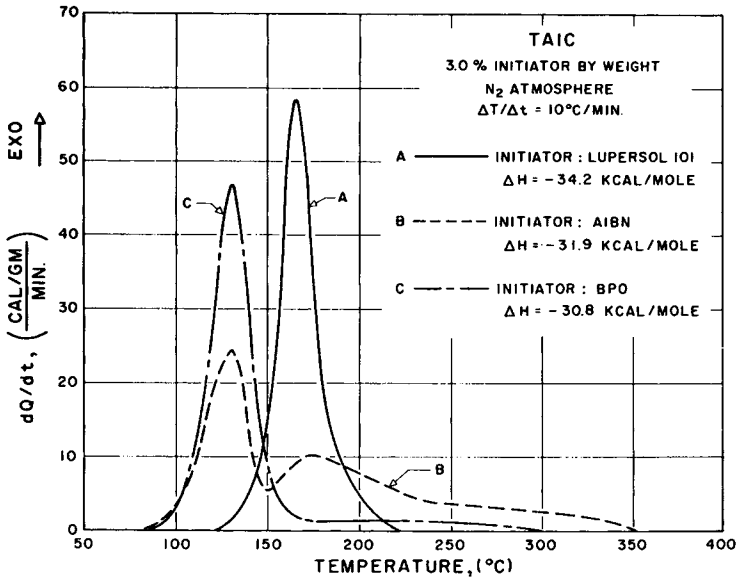

Fig. 9. Thermocalorimetry: polymerization of TAIC in nitrogen. Effect of initiator type.

the TAIC. The total heat of reaction is due to both radical-induced and thermal-induced polymerization. The heats of reactions, −30.8 kcal/mole for BPO and −31.9 kcal/mole for AIBN, are somewhat lower than that which was obtained for Lupersol 101, −34.2 kcal/mole (cf. uninitiated value, −27 kcal/mole).

For a 3.0% solution of Lupersol 101 in TAIC, the extent of reaction determined by calorimetry is about 62%. This value agrees with the results obtained by infrared analysis (Fig. 10 and Table III), for which the average conversion for five runs was 64.5 ± 3.1% (specimens quenched from 230°C).

TABLE III
Extents of Reaction During First Exotherm Measured by Infrared Analysis

Monomer (% initiator)	Extent of reaction of allyl groups, %
TAIC (3.0% Lupersol 101)	64.5 ± 3.1
TAC (no initiator, no air)	0.5
TAC (no initiator, air present)	11.2 ± 4.0
TAC (3.0% Lupersol 101)	79.6 ± 3.1
TAC (5.0% Lupersol 101)	81.0 ± 3.5

Radical-Induced Polymerization of TAC

Table II summarizes calorimetric experiments made with TAC (heat of initiator decomposition removed[9]). Reactions using various concentrations of Lupersol 101 are shown in Figure 11 for nitrogen and in Figure 12

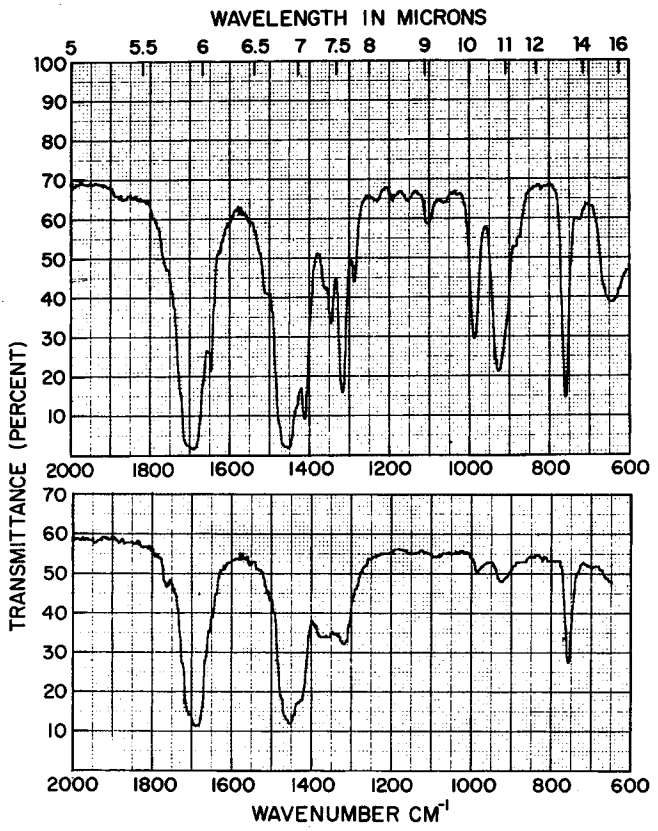

Fig. 10. Infrared spectra of TAIC with 3.0% Lupersol 101 (air atmosphere): (a) room temperature; (b) quenched from 220°C (note: ~64% conversion of double bonds to single bonds).

for air. Two separate thermal events are observed. The first is associated with radical-induced polymerization of TAC. In this first region, infrared spectra (Fig. 13) show loss of allyl unsaturation but no isomerization. The second event is associated with the isomerization of the poly(TAC) structure to that of poly(TAIC) with no further polymerization (by infrared analysis of the unreacted allyl groups of the TAIC). Infrared analysis (Fig. 13) shows that after the second thermal event, complete isomerization has taken place. The total heat in the first peak for a 3% solution of Lupersol 101 in TAC is −44.4 kcal/mole. This is a higher conversion than that which could be obtained from the thermal polymerization of TAIC (−27 kcal/mole); therefore, after isomerization occurs, no further polymerization results. The heat generated in the second peak is then only the heat of isomerization of poly(TAC) to poly(TAIC). For solutions with from 0.25% to 10.0% Lupersol 101 in TAC, the results are similar in that the first step is polymerization of TAC and the second is solely isomerization of poly(TAC) to poly(TAIC). As the level of initiator

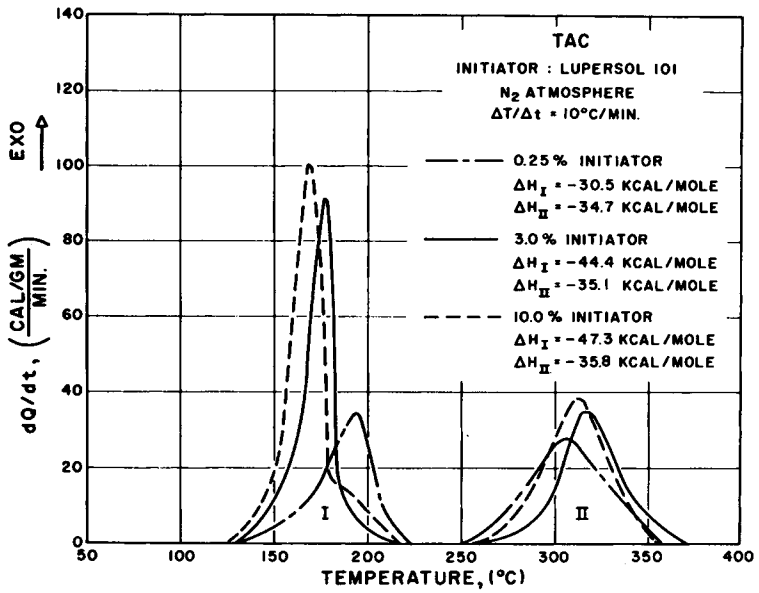

Fig. 11. Thermocalorimetry: polymerization of TAC in nitrogen. Effect of initiator concentration.

is increased, the amount of heat generated in the first step increases but the heat of isomerization remains the same, with $\Delta H = -34$ to -36 kcal/mole. There does not seem to be any effect of air on the reactions in this range. The 5.0% (not shown) and 10.0% solutions of Lupersol 101 in TAC exhibit the same shoulder on the lower reaction peak as do the 5.0% and 10.0% solutions of Lupersol 101 in TAIC, and again it is not affected by the presence of air. Decreasing the concentration to 0.1% Lupersol 101 (in nitrogen, Fig. 14) causes a change in the results. There is so little polymerization taking place in the first reaction step that when the TAC starts to isomerize, the newly formed TAIC thermally polymerizes. This also occurred when no initiator was used (Fig. 5).

For a 3.0% solution using the BPO (Table II), the polymerization reaction again begins at a lower temperature than it does with Lupersol 101. The total heat generated during the polymerization is again lower but the heat of isomerization remains the same at $\Delta H = -35$ kcal/mole.

Using the value of -55.5 kcal/mole for the heat of reaction if all the allyl groups react, then (Table II) there would be 80% conversion of the allyl groups for a 3.0% solution of Lupersol 101 in TAC. The infrared (Fig. 13 and Table III) and calorimetric results again agree. The average conversion for five infrared runs was 79.6 ± 3.1% (specimens quenched from 220°C).

Further Discussion

TAC polymerizes to a greater extent than does TAIC when the concentration of initiator is greater than about 0.5%. The conversions of both

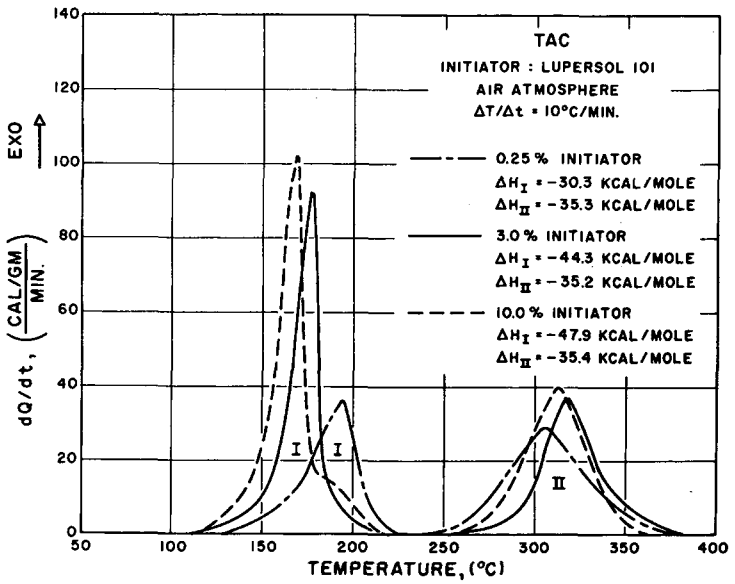

Fig. 12. Thermocalorimetry: polymerization of TAC in air. Effect of initiator concentration.

can be very high (>70%), and so much of the polymerization must occur in the solid or semisolid state. The high conversion and reaction in the solid state are facilitated by the length and flexibility of the allyl groups which can react intramolecularly to form a network of small rings. The smallest ring is seven-membered for TAIC and nine-membered for TAC. A reason for the higher conversion of TAC is the extra length and flexibility of its allyl groups.

Complete isomerization (as determined by infrared analysis) of the cyanurate to isocyanurate takes place under two conditions: (1) in the absence of initiator and air, the TAC monomer isomerizes before polymerizing, presumably by an intermediate which forms by intramolecular rearrangement of electrons (Fig. 15); (2) isomerization of poly(TAC) to poly(TAIC) also occurs. Isomerization by the intramolecular rearrangement of electrons depends on complete unsaturation of the three allyl groups, and this is not the case when TAC has polymerized. In order for isomerization to proceed by this mechanism, there must first be depolymerization to recover the allyl unsaturation. Depolymerization occurs when the polymer approaches the thermodynamic ceiling temperature where the polymer and monomer are in equilibrium. Heating poly(TAC) causes some monomer to form. The TAC then isomerizes by electron rearrangement to form TAIC. The depletion of the monomer TAC upsets the equilibrium of monomer and polymer and causes more monomer to form. The newly formed TAIC then thermally polymerizes to poly(TAIC). The net effect observed by infrared analysis and calorimetry is isomerization of poly(TAC) to poly(TAIC).

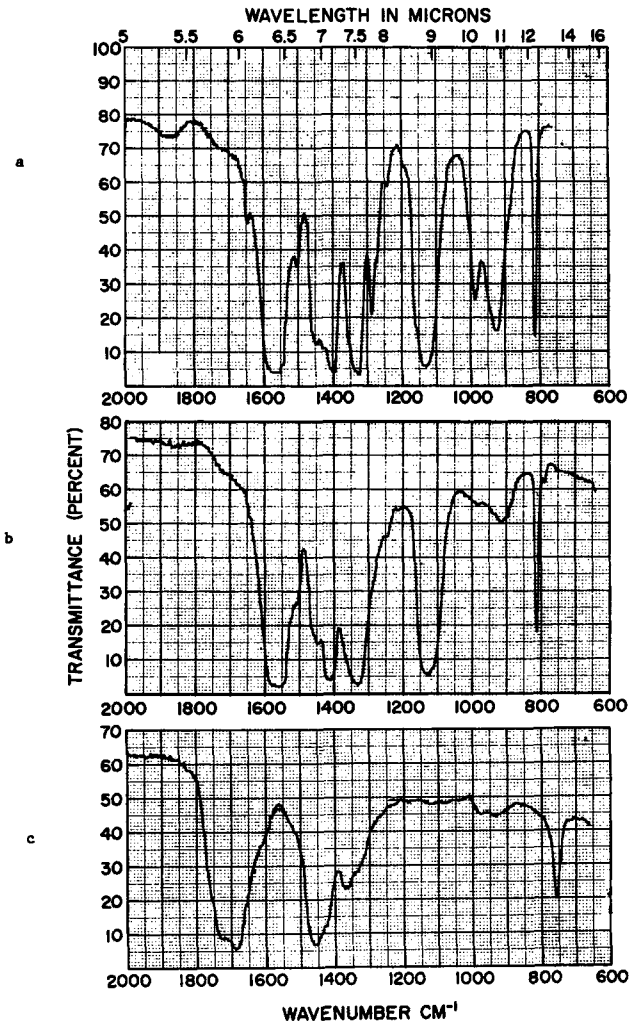

Fig. 13. Infrared spectra of TAC with 3.0% Lupersol 101 (air atmosphere): (a) room temperature; (b) quenched from 210°C (note: no isomerization; ~79% reaction of the allyl groups); (c) quenched from 390°C (note: complete isomerization of the TAC structure to that of TAIC).

The polymer resulting from isomerization should be poly(TAIC). Comparison of the TGA and DTA curves for poly(TAIC) and the isomerized poly(TAC) (Fig. 1) shows a substantial difference. The isomerized poly(TAC) decomposes at a much lower temperature than does poly(TAIC) (350° compared to 420°C). The TGA curve for poly(TAC) shows a weight loss beginning at 300°C. This weight loss occurs in the region where isomerization occurs, and the initial part of the weight loss is probably due to loss of monomer, TAC or TAIC, which is lost to the open system before it can repolymerize. This same TGA curve shows an inflection at 350° to

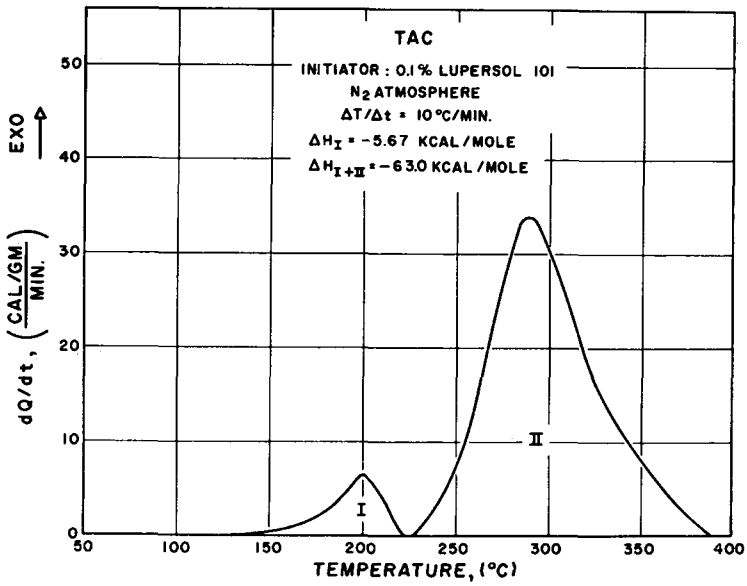

Fig. 14. Thermocalorimetry: polymerization of TAC in nitrogen. Initiator concentration = 0.1% Lupersol 101.

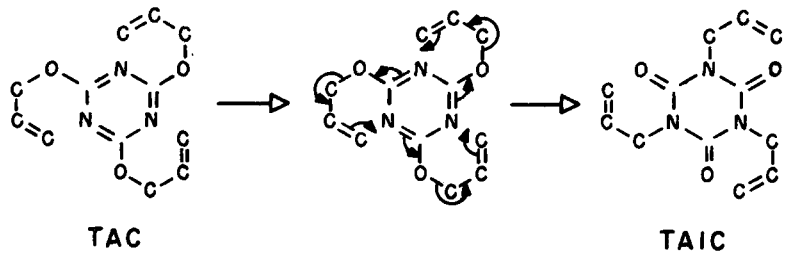

Fig. 15. Isomerization of triallyl cyanurate to triallyl isocyanurate.

375°C, indicating that another reaction is taking over. DTA curves of poly(TAC) show decomposition immediately following the isomerization. Since poly(TAIC) is thermally stable at these temperatures, the decomposition of isomerized poly(TAC) must be initiated by decomposition of poly(TAC) which has not isomerized as yet. Poly(TAC) contains a weaker linkage, the allyl ether linkage, than does poly(TAIC). Breakdown of the allyl ether linkage along with the highly exothermic nature of the isomerization reaction would cause the structure to decompose at a lower temperature than poly(TAIC).

Appendix

Development of the Basic Equation for the du Pont-Type DSC

A schematic of the instrument in linear coordinates is shown in Figure 16. The basic assumptions are: (1) The constantan disc is the primary means of heat transfer

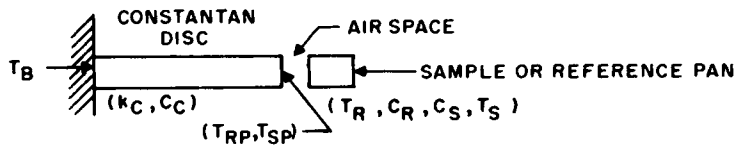

Fig. 16. Sketch of du Pont DSC constantan disc in linear coordinates: T_{RP}, T_{SP} = temperature of the reference and sample constantan platforms (temperatures measured by the instrument); T_R, T_S = temperature of the reference and sample pans; T_B = temperature of the thermal source; k_C = thermal conductivity of the constantan disc; and C_S, C_R, C_C = total heat capacity of the sample pan, reference pan, and constantan disc.

to and from the sample and reference pans. (2) There are no interactions between the sample and reference portions of the calorimeter. (3) All thermal resistances and heat capacities are independent of temperature. (4) The thermal losses along the disc are small compared to the heat flow along the disc. (5) The air space between the constantan disc and the sample and reference pans is small and the thermal losses and the heat needed to raise the temperature of this air space are also small and will be neglected.

Placing an energy balance around the sample or reference portion of the constantan disc yields

$$C_C \partial T/\partial t = k_C \partial^2 T/\partial x^2 + k_C \partial^2 T/\partial y^2 + k_C \partial^2 T/\partial z^2 \tag{1}$$

where T = the temperature of the disc.

Using the x-direction as the primary direction of heat flow and assumption (4), eq. (1) now becomes

$$C_C \partial T/\partial t = k_C \partial^2 T/\partial x^2. \tag{2}$$

This equation has been solved[11] assuming that for any given instant in time, the entire instrument is at steady state and therefore the $\partial T/\partial t$ for the disc is zero. This is not true, since the instrument is usually being programmed up in temperature at a given rate. It is better to assume that the temperature of the disc increases at a rate equal to the programming rate and therefore $\partial T/\partial t$ = constant. Equation (2) now becomes

$$d^2T/dx^2 = A \tag{3}$$

where $A = (C_C/k_C)(\partial T/\partial t)$ = constant.

Equation (3) has the general solution

$$T = C_1 + C_2 x + C_3 x^2 \tag{4}$$

where C_1, C_2, and C_3 are determined from the boundary conditions and the particular solution A. The boundary conditions for the sample portion of the constantan disc are

$$\text{B.C. 1: at } x = 0, \quad T = T_B$$

$$\text{B.C. 2: at } x = L, \quad q_{x=L} = q_S = C_S dT_S/dt + dh/dt + q_S'$$

where q_S is the net heat flow to the sample pan and goes to heating of the sample material and pan, to the thermal event, and to thermal losses (qs').

Solving eq. (3) for C_1, C_2, and C_3 yields

$$C_1 = T_B$$

$$C_2 = -[(C_S/k_C)dT_S/dt + (1/k_C)dh/dt + q_S'/k_C]$$

$$C_3 = A/2.$$

The general solution of eq. (3) for the sample portion of the disc is therefore

$$T = T_B - \left[\frac{C_S}{k_C}\frac{dT_S}{dt} + \frac{1}{k_C}\frac{dh}{dT} + \frac{q_S'}{k_C}\right]x + \frac{A}{2}x^2. \tag{5}$$

Solving this equation for the temperature at $x = L$ (measured temperature T_{SP}) yields

$$T_{SP} = T_B - R_C C_S \frac{dT_S}{dt} - \frac{R_C dh}{dt} - R_C q_S' + A' \tag{6}$$

where $R_C = L/k_C$ = resistance to heat flow along the disc; $A' = L^2A/2$ = constant.

The boundary conditions for the reference portion of constantan disc are

$$\text{B.C. 1: at } x = 0, \qquad T = T_B$$

$$\text{B.C. 2: at } x = L, \qquad q_{x=L} = q_R = C_R dT_R/dt + q_R'$$

where q_R is the net heat flow to the reference pan and goes to heat the reference material and pan and to thermal losses.

Solving eq. (3) for the temperature of the reference portion of the disc as a function of distance yields

$$T = T_B - \left[\frac{C_R}{k_C}\frac{dT_R}{dt} + \frac{q_R'}{k_C}\right]x + \frac{A}{2}x^2. \tag{7}$$

The temperature at $x = L$ or T_{RP} is

$$T_{RP} = T_B - R_C C_R \frac{dT_R}{dt} - R_C q_R' + A'. \tag{8}$$

The response of the du Pont DSC is the temperature difference between the sample and reference platforms on the constantan disc or $T_{RP} - T_{SP}$. Subtracting eq. (6) from eq. (8) and adding and subtracting $R_C C_S dT_R/dt$ from the left hand side yields

$$\underset{\text{I}}{T_{RP} - T_{SP}} = \underset{\text{II}}{R_C(C_S - C_R)\frac{dT_R}{dt}} + \underset{\text{III}}{R_C\frac{dh}{dt}} - \underset{\text{IV}}{R_C C_S d\frac{(T_R - T_S)}{dt}} + \underset{\text{V}}{R_C[q_S' - q_R']}. \tag{9}$$

The last term in eq. (9) (IV) is due to the difference in thermal losses (convection and radiation) between the sample and reference plans which are at slightly different temperatures. In general, the temperature difference between the sample and reference pans is small, and therefore difference in thermal losses will also be small and will be neglected.

The quantity $T_R - T_S$ in term III is not known. An expression for $T_R - T_S$ in terms of the measurable temperatures T_{RP} and T_{SP} can be developed by solving eq. (3) with different but equivalent boundary conditions. It has been assumed that the heat leaving the constantan platform is equal to the heat entering the sample or reference pan; therefore, from Fourier's law,

Reference:

$$q_{x=L} = \frac{T_{RP} - T_R}{R_R}$$

Sample:

$$q_{x=L} = \frac{T_{SP} - T_S}{R_S}.$$

R_R, R_S = thermal resistance of air spaces to heat flow.

The new boundary conditions are now
Reference:

$$x = 0 \quad T = T_B$$

$$x = L \quad q_{X=L} = \frac{T_{RP} - T_R}{R_R}$$

Sample:

$$x = 0 \qquad T = T_B$$

$$x = L \quad q_{x=L} = \frac{T_{SP} - T_S}{R_S}.$$

Solving eq. (3) for the temperature along the x-axis,
Reference:

$$T = T_B - \frac{1}{k_C}\frac{T_{RP} - T_R}{R_R}x + \frac{A}{2}x^2 \tag{10}$$

Sample:

$$T = T_B - \frac{1}{k_C}\frac{T_{SP} - T_S}{R_S}x + \frac{A}{2}x^2. \tag{11}$$

Solving for the temperature at $x = L$,
Reference:

$$T_{RP} = T_B - \frac{R_C}{R_R}(T_{RP} - T_R) + A' \tag{12}$$

Sample:

$$T_{SP} = T_B - \frac{R_C}{R_R}(T_{SP} - T_S) + A'. \tag{13}$$

Solving the equations for T_R and T_S and subtracting yields

$$T_R - T_S = \frac{R_C + R_R}{R_C}T_{RP} - \frac{R_C + R_S}{R_C}T_{SP} - \frac{R_R - R_S}{R_C}T_B - \frac{R_R - R_S}{R_C}A'. \tag{14}$$

Adding and subtracting $\left(\frac{R_C + R_S}{R_C}\right)T_{RP}$ to the left-hand side and taking the derivative of $T_R - T_S$ with respect to time yields

$$\frac{d(T_P - T_S)}{dt} = \frac{R_C + R_S}{R_C}\frac{d(T_{RP} - T_{SP})}{dt} - \frac{R_R - R_S}{R_C}\left[\frac{dT_{RP}}{dt} - \frac{dT_B}{dt}\right]. \tag{15}$$

This value can now be substituted into eq. (11):

$$\underset{\text{I}}{T_{RP} - T_{SP}} = \underset{\text{II}}{R_C(C_S - C_R)\frac{dT_R}{dt} + R_C\frac{dh}{dt}}$$

$$\underset{\text{III}}{- (R_C + R_S)C_S\frac{d(T_{RP} - T_{SP})}{dt}} \underset{\text{IV}}{- (R_C + R_S)\left[\frac{dT_{RP}}{dt} - \frac{dT_B}{dt}\right]}. \tag{16}$$

The last term (IV) in eq. (16) is equal to zero since the temperatures T_{RP} and T_B are both on the constantan disc, and it was assumed that the rate of temperature increase along the disc was a constant. In actual practice this is not true, since there is a temperature fluctuation along the disc. This last term also contains the difference between two resistances R_S and R_R. Through proper instrument design, these two resistances are approximately equal. Therefore, the last term in eq. (16) is the product of two small values and can be neglected.

Equation (16) now becomes

$$R_{RP} - T_{SP} = R_C(C_S - C_R)\frac{dT_R}{dt} + R_C\frac{dh}{dt} - (R_C + R_S)C_S\frac{d(T_{RP} - T_{SP})}{dt}. \quad (17)$$

This equation is that used to describe the response of the du Pont DSC.

The partial support of this project by NASA (Research Grant NGR 31-00-221) is acknowledged.

References

1. R. N. Castle, *Heterocyclic Chemistry*, Interscience, New York, 1969, p. 64.
2. G. W. Wheland, *Resonance in Organic Chemistry*, Wiley, New York, 1955, pp. 89–109.
3. du Pont 900 DTA Instruction Manual, E. I. du Pont de Nemours & Co., Instrument Products Division, Wilmington, Delaware.
4. B. H. Clampitt, D. E. German, and J. R. Galli, *J. Polym. Sci.*, **27**, 515 (1958).
5. D. E. German, B. H. Clampitt, and J. R. Galli, *J. Polym. Sci.*, **38**, 433 (1959). and H. F. Mark, NG. Gaylord.
6. B. H. Clampitt and A. P. Mueller, *J. Polym. Sci.*, **62**, 15 (1962).
7. J. K. Gillham, in *Encyclopedia of Polymer Science and Technology*, Vol. 1, H. F. Mark, N. G. Gaylord and H. M. Bikales, Eds., Wiley, New York, 1964, pp. 760–770.
8. W. P. Brennan, B. Miller, and J. Whitwell, *Ind. Eng. Chem. Fundam.*, **8**, 313 (1969).
9. C. C. Mentzer, Ph.D. Thesis, Chemical Engineering Department, Princeton University, 1972.
10. K. J. Ivin in *Polymer Handbook*, J. Brandrup and E. H. Immergut, Eds., Interscience, New York, 1966, pp. 363–398.
11. R. A. Baxter in *Thermal Analysis*, Vol. 1, R. F. Schwenker Jr. and P. O. Garn, Eds., Academic Press, New York, 1969, pp. 65–84.

Received January 6, 1972
Revised August 30, 1972